ISSN (Print) : 0974-6846
Indian Journal of Science and Technology, *Vol 8(31), DOI: 10.17485/ijst/2015/v8i31/84419, November 2015* ISSN (Online) : 0974-5645

Temperature Prediction using Finite Element Modeling on Friction Stir Welding of AA6061-AZ61

L. A. Kumaraswami Dhas[1*], D. Raguraman[2], D. Muruganandam[3] and B. Senthilkumar[3]

[1]Department of Mining Machinery Engineering, Indian School of Mines, Dhanbad-826 004, Jharkhand, India; lakdhas1978@gmail.com

[2]Department of Production Engineering, Sri Sairam Engineering College, Chennai-600 044, Tamil Nadu, India; raguraman150807@gmail.com,murudurai@gmail.com, bsenthilme@gmail.com

Abstract

Background/Objectives: The objective of this paper is on developing a thermo-mechanical model to predict the thermal histories of the FSW butt joint of AA 6061-AZ61. **Methods/Statistical Analysis**: The FEM model is developed for the temperature and residual stress characteristics of the weld material. The friction serves as the heat source which exists between the pin and plate as well as the shoulder and plate. To understand the dynamics of the Friction Stir Welding thermal and residual effects,the thermal history and the evolution of longitudinal, lateral residual stresses in the friction stirred weld are simulated using ANSYS. **Findings**: The temperature influences on Von-mises stress and strain on the different zones are analyzed. The contour technique using Coordinate Measuring Machine (CMM) is used to measure the residual stress of the welded plate.It is found that the proposed model is correlated with experimental result. **Application/ Improvements**: The developed FEM model can be used as one of the tool for correlating the temperature and residual stresses on the weld zone. The CMM also can be used to predict the residual stresses through contour measurement.

Keywords: Finite Element Method, Friction Stir Welding, Residual Stress, Temperature Distribution,Thermo-Mechanical Model

1. Introduction

Advanced joining technology is the current research interest in the manufacturing processes of light weight structures.The design of lightweight structures like aircraft panels and vehicle body shells can be welded effectively. Considerable effort by researchers has been made to develop various joining processes and their assessment on suitability for use in lightweight structures[1–5].

Apart from the advantages of FSW as a new welding technique for welding dissimilar alloys, the knowledge of temperature gradient and residual stresses are still not completely understood. It is well known that the residual stresses of the weld will negatively affects the fatigue character and anti corrosion effects[6,7]. Several investigations of the residual stress distribution in FSW weld were conducted by experimental methods.

Webster et al.[8] reported a measurement of residual stress in FSW welded Al 7108 by the synchrotron X-ray technique,which shows that the longitudinal residual stress varies in the range from 60 to 140 MPa and also shows a correlation between the detailed residual stress features and the heat flow in the weld. Sutton et al.[9] investigated the residual stress in 2024-T3 aluminum friction stir butt welds using the neutron diffraction technique and the results show that the highest stresses occur near the crown side of the weld over the entire FSW region.

To gain physical perception of the Friction Stir Welding process and the prediction of the residual stresses, it is a need to develop numeric models or simulation. It will also be advantageous that developed model (s)/simulation used to minimize the residual stresses in the weld. The developed method with optimal parameters will guide the

* *Author for correspondence*

implementation of the process. Song and Kovacevic have studied the heat transfer in FSW using the finite difference method[10,11]. Few papers have directly involved with the modeling of the thermo-mechanical stress analysis in FSW. Chao[12] proposed a model to predict the thermal history and the subsequent thermal stress and distortion of the workpiece without involving the mechanical effect of the tool. Dong[13] developed several models to separately deal with the subproblems of heat transfer, material flow and plastic flow. From the point of physics for the FSW process, the mechanical effect of the tool needs to be included into the thermomechanical model.

The Finite Element Method (FEM) is proposed for model on this paper to study the thermal impact and evolution of the residual stresses in the weld and tool. This study is accomplished by parametrically studying the effects of varying welding parameters, primarily the traverse speed of the tool. The entire welding process is simulated using the commercial finite element package ANSYS. Experiments on a welding of Al 6061-T6 and AZ61 are also carried out. The temperature history and the residual stresses for the welded plates are measured by the contour technique for a comparison with the calculated results.

1.1 Model Description

1.1.1 Heat Transfer Model

The heat transfer in FSW contains conduction, convection and radiation. The governing equation for transient heat transfer analysis during the FSW process is given as follows:

$$\rho C\frac{\partial T}{\partial t}=\frac{\partial}{\partial x}(K\frac{\partial T}{\partial x})+Q_{pd}+Q_{pin} \quad (1)$$

Where, p is the density of material; C is the specific heat capacity; K is the thermal conductivity of the workpiece; The term Q_{pd} is the heatgeneration rate caused by plastic deformation in the work piece far from the interface and Q_{pin} is heat generation at the tool's pin side with workpiece interface that are inserted as a rate per unit volume at near the tool pin. The heat generated at the interface between horizontal surfaces of the tool (shoulder and pin tip) will be applied as a boundary condition.

The friction between the rotating tool and the base metals to be welded is considered as the main heat source in Friction Stir Welding. Considering an elemental friction at the contact surface between the tool shoulder and the top surface of base metal, the rate of heat generation derived in the element at radius r is:

$$dQ=2\pi\omega r^2\mu(T)p(T)dr \quad (2)$$

The heat generation rate over the entire interface of the contact on the pin surface will be:

$$Q=\int_0^{R_p}2\pi\omega r^2\mu(T)p(T)dr=\frac{2}{3}\pi\omega\mu(T)p(T)R_p^3 \quad (3)$$

The rate of heat generation at shoulder and the top surface of the base metal is a function of the angular velocity w, coefficient of friction m and radius r. As the m (T) and p (T) are dependent on the local temperature and the radius r, Equation 3 is difficult to evaluate. The coefficient of friction is expected to decrease as the temperature increases and the plastic deformation increases. A constant value of the coefficient of friction is used to approximate the comprehensive effect of plastic and thermal effects during Friction Stir Welding. The predicted temperature gradients are verified with the measured temperature values. The heat generation in the surface area of the probe is considered the same as that of the shoulder surface area with a radius equal to that of the probe.

1.1.2 Mechanical Model

The force equilibrium on an arbitrary volume results in the following governing equation known as the equilibrium equation:

$$Div(\Omega)+F_V=\rho.a \quad (4)$$

Where'Ω is the stress tensor, p is the equivalent density, a is the acceleration and F_V is the volume force intensity.

The inertia effect is neglected in this model since a constant rotational speed and a constant longitudinal speedare used during FSW.

In the displacement formulation, the essential boundary conditions are specified as follows: For the clamed portion of the plate surface and the normal displacement,

$U = 0$ (5)

For the bottom of the plate at $y = 0$,

$Uy = 0$ (6)

1.1.3 Finite Element Model

The ANSYS 14 is used as a commercial FEM software to carry out the numerical simulation. For the prediction

of temperature and multi-linear strain hardening effects Lagranrian's model is incorporated in this simulation. The element topology used is eight nodes and has stress stiffening, plasticity, large strain capabilities and large deflection[14].

Symmetry along the weld line is assumed in the numerical evaluation, so the welded plate is meshed with a total of 12649 nodes. The moving heat sources of the pin and the shoulder are represented as moving nodes of the heat generation in each computational time step. The relatively larger contact region of the shoulder and the work piece is expected to contribute a large part of the mechanical stress, especially in the upper half part of the weld. The temperature gradient is large around the welding zone and seriously changes the materials properties. In order to increase the accuracy of the mechanical solution, the thermal and mechanical solutions are coupled with the temperature data at each increment time and is used to evaluate the mechanical properties and the thermal parameters.

2. Experimental Setup

2.1 FSW implementation

The 6061-T6 Al alloy plates and AZ61 plates, each with a dimension of 100 x 50 x 6 mm are butt welded in the Friction Stir Welding machine. The schematic sketch of the Friction Stir Welding process is shown in Figure 1.

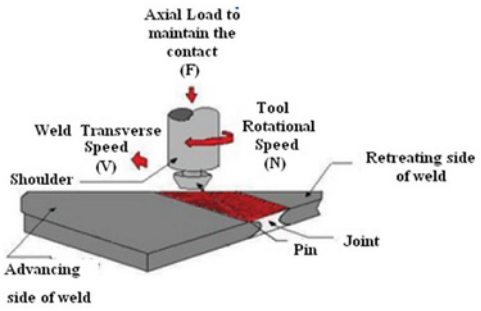

Figure 1. Schematic illustration of friction stir welding process.

In this experimental work, ten thermal couples are embedded in retreating side of plate on which five are located 1.2 mm below the upper surface and the other five are located 1.2 mm from the root surface, with a distance of 12, 15, 18 and 21 mm respectively from the weld nugget. The gap between the thermocouples in the longitudinal direction is 12 mm. A micrometer measurement unit attached with sensor is used to monitor the plunge depth of the tool. Temperatures are acquired and recorded in a time-duration of 100 milli seconds by a LABVIEW. The specimens, each having dimensions of 25 x 25 mm are cut with a waterjet cutting machine and are subsequently polished. To minimize the mechanical effect induced by the sample polishing at least 0.015 mm depth of the outer layer of the specimen was etched away with Keller's reagent.

2.2 Residual Stress Measurement using CMM

To determine the residual stress over a cross-section contour method can be used. The contour method is working with the principle that when a work material is cut into two halves along a straight line and the cut portions will deform as the residual stresses normal to the surface are released during cutting. The deformations of the cut portions can be measured as contour measurement technique and helps to determine the initial residual stress on the cut plane. The contour method is being unique as it provides a full two dimensional details of the residual stress component normal to the cross section[15,16]. From References[15,16], main procedures of the contour method include: 1. specimen preparation by cutting, 2. contour measurement, 3. data processing and 4.finite element analysis to determine residual stress.

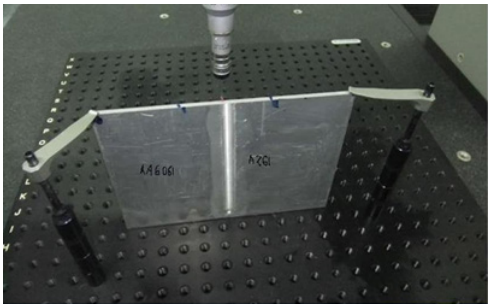

Figure 2. Contour measurement using CMM.

The measurement of the weld surfaces in the present study was performed using a HEXAGON GLOBAL Coordinate Measuring Machine (CMM). The selection of point spacing is very important for the profile measurement of the weld surface. For the stress measurement in the weldment, both halves of the welds were measured with a point spacing of approximately 0.5 mm in the transverse as well as axial directions of tool

and in the weld region a dense point spacing of 0.25 mm was used[17]. In Reference[18], the measurement points were designed in a fashion with 1 mm increment. For 6 mm thick specimen, the 0.5 mm point spacing is applied for entire cut portions. The contour measurement is shown in Figure 2, the measured raw data for 6 mm thick specimens are shown in Figure 3.

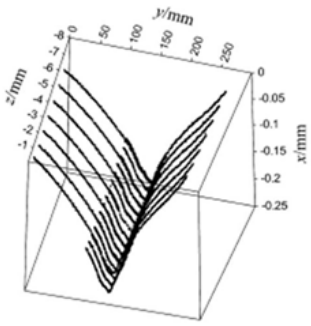

Figure 3. Contour measurement data from CMM for the weld surface.

The most important criterion on data analysis is the alignment of measured data with the average of the two sets of measurements as it is essential to remove shear stress effects on cutting imperfections.

3. Result and Discussion

3.1 Typical Microstructure of the FSW Weld

The micro structure of the weld is resulted from a dynamics of the physical process and is strongly relevant to the history of thermal effects and/or the plastic deformation on the weld region. The residual stress distribution is affected due to temperature distribution and plastic deformation.

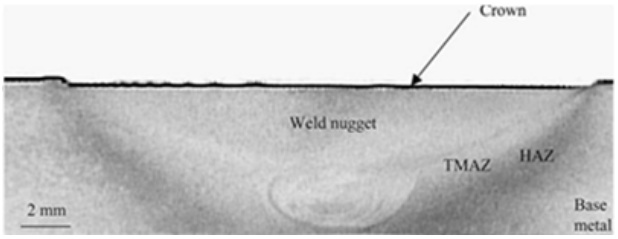

Figure 4. Optical micrograph for the weld surface.

Figure 4 shows a typical optical micro graph taken from the prepared specimen for metallography. The optical micro-graph reveals four unique regions: 1. Nugget Zone (NZ); 2. Thermo-Mechanically Affected Zone (TMAZ); 3. Heat Affected Zone (HAZ); and 4. The base metal. In the NZ, the refined grains get equiaxed and are responsible to the dynamic re-crystallization. The HAZ usually contains a vast amount of coarsened grains with relatively lesser yield strength than that in the NZ and the TMAZ.

3.2 Study of Temperature–Time History in FSW

Figure 5 shows the temperature and temperature gradient contours in the cross-section perpendicular to the welding direction. In the Nugget Zone the highest temperature is observed from the lateral surface of shoulder to the pin root side as the rotation of the shoulder and pin contacts with the plate and responsible for higher heat flux. The relative heat generation and dissipation at the contact surfaces causes the temperature contour in the NZ to make a "V" shape of distribution.

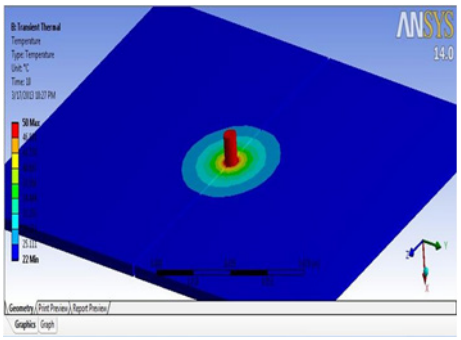

Figure 5. Temperature gradient with the loading of pin and its transient flow on z-direction (V = 100 mm/min, ω = 800 rpm).

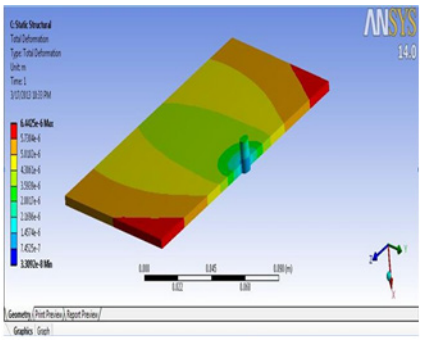

Figure 6. Temperature gradient with the loading of pin and its transient flow on y-direction (V = 100 mm/min, ω = 800 rpm).

Figure 6 shows that the maximum temperature gradient in the lateral direction (y-direction) observed in the region nearer to the edge of the shoulder.

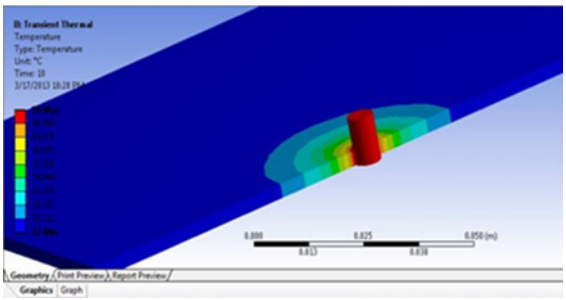

Figure 7. Contour Temperature gradient with the loading of pin and its transient flow on x-direction (V = 100 mm/min, ω = 800 rpm).

The highest heat generation in the NZ region and the highest heat dissipation from the NZ region to nearby shoulder edge contact regions. The temperature gradient contours in the x-direction (longitudinal direction) on the upper surface during welding are revealed in Figure 7, which proves that the region contacted with the lateral surface of the shoulder is subjected to the higher temperature gradient effect. It is believed that the "V"-type of temperature gradient distribution in the weld zones contributes to coarsening of grains in the HAZ and the TMAZ shown in Figure 4.

Figure 8 shows a comparison of the calculated and the measured temperature–time history at the location 10 mm to the weld center-line and 1.6 mm below the upper surface of the weld plate. The respective rotational and the traverse speeds of the tool are 500 rpm and 140 mm/min.

In the beginning stage of the welding, the calculated values are higher than the measured values, but they are lesser than the measured values once the maximum temperature is reached, which may be due to the assumption for the backing plate's constant temperature. Actually, the temperature of the backing plate rises because of the rise in heat during welding and the decrements of cooling rate in the later stage of welding. However, the calculated temperature gradient values are in a reasonable agreement with the measured ones for the entire welding process.

Figure 8 (b) shows a temperature distribution along the lateral direction (for nodes 1.6 mm below the top surface of the plate) at the impact when the shoulder's center is passing over this location. It is clear that there is a decrement of temperature when there is a increments of the traverse speed especially in the weld zone. A good agreement between the measured and calculated temperature gradient values implies that this developed model can be used for the prediction of temperature history.

3.3 Analysis of Stress Distribution in the Weld

The residual stresses will be raised in the weld zones during welding due to contraction during the cooling of the welds. Furthermore, the combined transverse and the rotational movements of the tool will cause additional stresses in the weld zone due to the mechanical constraints by the fixture on the weld plates .

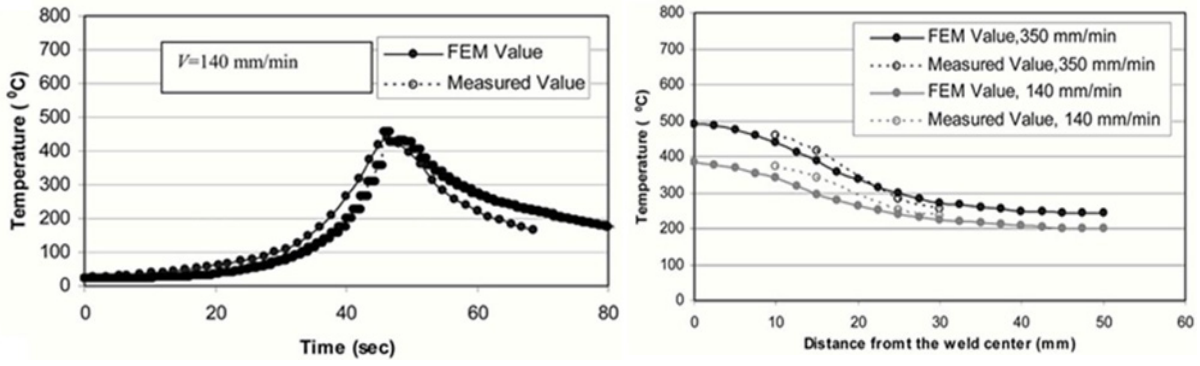

(a) (b)

Figure 8. A comparison of the calculated and measured temperature history. (a) Temperature – time profile for the location 15 mm to the weld centre line (V = 100 mm/min, ω = 800 rpm). (b) Temperature profle along the weld nugget to HAZ distance.

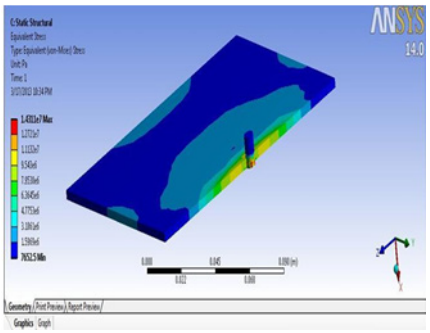

Figure 9. Predicted three-dimensional residual stress distribution in the welded plate. (V = 100 mm/min, ω = 800 rpm).

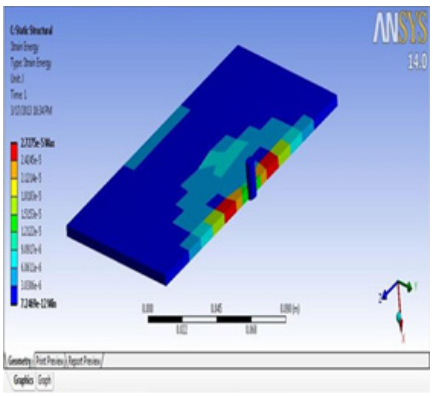

Figure 10. Predicted residual stress contour in the welded plate perpendicular to the cross section AA. (V = 100 mm/min, ω = 800 rpm).

Figure 9 shows the residual stress contours in all three x-y-z directions of the welded plate. The predicted stress distribution in Figure 10 is like the one encountered in steel welds and also complies with measurements on friction stir welded AA 6061- AZ61 with the cut compliance method reported by Dalle Donne, et al.[6]. It is noticed that the initial contact portion and final relieving portion of the weld have different stress distributions as compared with the nugget zone of the plate, which may be caused by the variation in the correlated thermo-mechanical process during the welding. At the end of the weld, the tool is lifted up and it leaves the keyhole above the weld region due to compression stress.

4. Conclusion

A three-dimensional modeling and measurement of the temperature and stress evolution in the FSW of 6061-T6 Al alloy and AZ 61 Magnesium alloy is conducted and the experimental values validate the efficiency of the proposed model. The prediction and measurement shows that the maximum temperature gradients in longitudinal and lateral directions are located just beyond the limits of shoulder edge and also shows that the longitudinal residual stress is greater than the lateral residual stress at the upper surface of the weld.

The prediction implies that the higher stress is located in the region from top surface of weld zones to the mid depth of the weld plate.

A higher traverse speed forces a more accumulation of high longitudinal stresses and a minor amount lateral stress field in the weld zone, which make agreements with the previously reported measurements with the neutron techniques. Further development of the FSW requires further research of the mechanical action of the probe and the fixture condition to the residual stress distribution on the weld zones.

5. References

1. He X, Gu F, Ball A. Recent development in finite element analysis of self-piercing riveted joints. International Journalof Advanced Manufacturing Technology. 2012 Jan; 58(5):643–9.
2. He X. Finite element analysis of laser welding: A state of art review. Material Manufacturing Process. 2012; 27(12):1354–65.
3. He X. A review of finite element analysis of adhesively bonded joints. International Journalof Adhesion and Adhesives. 2011 Jun; 31(4):248–64.
4. He X. Recent development in finite element analysis of clinched joints. International Journal of Advanced Manufacturing Technology. 2010 May; 48(5):607–12.
5. He X, PearsonI, Young K. Self-pierce riveting for sheet materials: State of the art. Journal of Material Processing Technology. 2008 Apr; 199(1-3):27–36.
6. Dalle Donne C, Biallas G, Ghidini T, Raimbeaux G. Effect of welding imperfections and residual stresses on the fatigue crack propagation in friction stir welded joints.In: Second International Symposium on Friction Stir Welding;Gothenburg, Sweden: TWI; 2000 Jun 26–8.
7. Zucchi F, Trabanelli G, Grassi V. Pitting and stress corrosion cracking resistance of friction stir welded AA 5083. Materials Corrosion. 2001 Nov; 52(11):853–9.
8. Webster PJ, Djapic OL, Browne PA, Hughes DJ, Kang WP, Withers PJ, Vaughan GBM. Synchrotron X-ray residual strain scanning of a friction stir weld. Journal of Strain Analysis. 2001 Jan; 36(1):61–70.
9. Sutton MA, Reynolds AP, Wang DQ, Hubbard CR. A study of residual stresses and microstructure in 2024-T3 aluminum friction stir butt welds. Journal of Engineering Materials and Technology. ASME. 2002 Mar; 124(4):215–21.

10. Song M, Kovacevic R.Thermal modeling of friction stir welding in a moving coordinate and its validation. International Journal of Machine Tool and Manufacturing. 2003 May; 43(6):605–15.
11. Song M, Kovacevic R. Numerical simulation and experimental analysis of heat transfer process in friction stir welding process. Proceeding of Institution of Mechanical Engineers, Part B, Journal of Engineering Manufacture.2003 Jan; 217(1):p. 73–85.
12. Cao Y, QiX. Thermal and thermo-mechanical modeling of friction stir welding of aluminum alloy 6001-T6. Journal of Materials Processing and Manufacturing Science. 1998: 7(10):215–33.
13. Dong P, Lu F, Hong JK, Cao Z. Coupled thermomechanical analysis of friction stir welding process using simplified models. Science and Technology of Welding and Joining. 2001 Oct; 6(5):281–7.
14. Alcan. Handbook of Aluminum.Alcan Aluminum Corporation; 3rd edition 1970.
15. Prime MB. Cross-sectional mapping of residual stresses by measuring the surface contour after a cut. Journal of Engineering Materials Technology. 2000 Nov; 123(2):162–8.
16. Prime MB, Sebring RJ, Edwards JM, Hughes DJ, Webster PJ. Laser surfacecontouring and spline data-smoothing for residual stress measurement. Experimental Mechanics. 2004 Apr; 44(2):176–84.
17. Dewald AT, Rankin JE, Hill MR, Lee MJ, Chen HL. Assessment of tensile residual stress mitigation in alloy 22 welds due to laser peening. Journal of Engineering Materials Technology. 2004 Nov; 126(4):465–73.
18. Zhang Y, Ganguly S, Edwards L, Fitzpatrick ME. Cross-sectional mapping of residual stresses in a VPPA weld using the contour method. Acta materialia. 2004 Oct; 52(17):5225–32.